Characterizing the mineralogical variability of a Chilean copper deposit using plurigaussian simulations

by J. Betzhold*, and C. Roth†

Synopsis

Knowing more about an orebody makes it easier to exploit it profitably. Many orebodies are made up of different rock types, alteration zones or mineralogical ensembles: oxides versus sulphides or facies with different metallurgical properties for example. Being able to model the spatial layout of these different facies is vital to good mine planning and management. Kriging cannot be used to generate numerical models of orebodies with complex geometric patterns because it gives too smooth an image. Over-smoothing has the meaning of changing the natural selectivity. Conditional simulations are required to do this kind of model respecting the natural variability: honouring the natural selectivity, dilution and ore loss.

Standard geostatistical simulations cannot duplicate many of the complex spatial relationships seen in the earth sciences, such as differently orientated facies, sets of conjugate veins or ore types where certain facies cannot touch. After a presentation of the case study, it will be shown why traditional methods for simulating indicators like the sequential indicator simulations, or the truncated gaussian method, cannot be used to simulate it. Plurigaussian simulations are then introduced and shown to be more powerful than the previous methods in their range of application. This is confirmed by the case study treated; a Chilean copper deposit, for which the plurigaussian simulations are seen to respect the different orientations of the individual facies as well as honouring the facies seen in drill holes, and respecting the proportion of each facies even if this varies in space (e.g. increases or decreases with depth).

Key words: geostatistics, indicators, conditional simulation, plurigaussian method, copper variability.

Introduction

The Mantos Blancos copper mine in north Chile has two metallurgical plants: one is a leaching and EW-SX plant for the oxides, and the second is a flotation plant recovering the sulphides. To obtain maximal recovery rates, the ore arriving at each of the plants should be of a previously known mineralogical composition and grade. Currently this is not easy to schedule from the mine, as the ore is quite variable in both mineralogical composition and grade.

The oxide ore distribution is controlled by elevation and proximity to the numerous existing faults. Sulphides, on the other hand, are spatially distributed according to mineralogical ensembles: chalcosite-bornite, chalcopyrite, chalcopyrite-pyrite, pyrite, and atacamite-malachite in the oxide zone. However, each of these mineralogical ensembles has its own particular grade range and metallurgical behaviour. This means that the recovery rates are not only variable but also highly dependent on the mineralogical ensemble being treated. In the same way the grades of the concentrate grades are also strongly dependent on mineralogical facies. For example, while chalcopyrite is easy to recover by flotation, the resulting concentrate is a low-grade product which of course affects the ultimate realization cost for the metallic copper. The preferred blend at the plant head would be one whose properties are constant in time. This means that the grade and recovery rates would be predictable, thus leading to a metallurgical product whose properties are equally predictable.

Currently it is not possible to extract the same type of ore, or mineralogical ensemble, as constant mill feed to limit this short-term variability in copper grades at the plant head, because of the erratic spatial layout of the different mineralized facies relative to the open pit selectivity. While a certain amount of selectivity is incorporated in the mining method, the irregularity of the limits between the different facies makes it impossible to stay within one lithological unit during the extraction process. A stocking and retrieving procedure (i.e. homogenizing) needs to be put into place to minimize the variability of the ore sent to the mill given the selectivity of the *in situ* ore.

* *Anglo American Corporation of South Africa Limited, 44 Main Street, Johannesburg, South Africa 2107.*

† *Centre de Géostatistique, 35 rue Saint Honoré, 77305 Fontainebleau, France.*

 SA ISSN 0038–223X/3.00 + 0.00. Paper received Jan. 1999; revised paper received Dec. 1999.

Such a procedure can only be formulated if one has access to a realistic image of the facies of the orebody. Kriging cannot give this realistic image, as the kriged estimate is a smoothed version of the reality. Only simulation techniques can reproduce the experimental variability while also respecting the experimental mineralogical ensembles. This paper focuses on how to simulate the facies, that is the geometry of the geology at the Mantos Blancos mine. The resulting simulations can then be used to best formulate a set of procedures so as to minimize the fluctuations of copper grades and mineralized ensembles at the mill head. To simulate the different facies indicator variables are simulated, where each indicator corresponds to the presence or absence of a given facies, or rock type in other cases.

The commonly used techniques for simulating indicators that could be applied to orebodies are sequential indicator simulations[1,2] and the truncated gaussian method[3,4,5]. When the geometry of the orebody is relatively simple, like banded sedimentary deposits, these methods could be considered. However, their application to more complex orebodies like Mantos Blancos is impossible because of the spatial order of the geology, that is, the relative position of the different facies as determined by the genesis of the orebody. In this case, only the plurigaussian simulation method can be applied successfully.

The theory behind the plurigaussian simulation method has previously been presented in detail[6,7,8]. In this paper, only an outline of the technique is provided. The focus will be on its application to characterizing the spatial variability of the different geological zones within the Mantos Blancos orebody, beginning with a description of the local geology.

Location, geological background and data

The orebody is located in the north of Chile, 45km north-east of the city of Antofagasta (cf. Figure 1). Rocks in the Mantos Blancos district are made of a volcanic sequence consisting of three major units which, from top to bottom are: andesitic flows and flow breccia, flow-breccia and flows of porphiritic dacite, and flows of augen (quartz-eye) dacite. The sequence dips to the south-west at 10–20° in the mine area. The mineralization, as confined to the dacite units, forms an irregular 100–200 m thick blanket that cuts the stratification at a slight angle.

The upper part of the blanket is oxidized, and the ore mineralogy consists of atacamite, chrysocolla and minor malachite. Otherwise, the blanket consists of steel-grey hard chalcocite that is often replaced by covellite with varying amounts of bornite. A second level below is mainly bornite with some chalcopyrite and galena in places. Below the previous galena zones there is generally a sharp change to chalcopyrite-pyrite mineralization, though in some places bornite grades to bornite-chalcopyrite, then to chalcopyrite or chalcopyrite-pyrite only. Rarely does chalcopyrite occur in sufficient quantities to give ore-grade mineralization. The limits of the chalcocite-bornite zone are used to define the economic mineralization. This contact between ore-grade and waste is sharp. Figure 2 shows a typical section from within the mine area.

To define the stocking and retrieving procedure the spatial variability of the grade within the deposit must be characterized under the assumption that the concentrate grade is constant within the different mineralogical ensembles. Therefore only the spatial variability of these ensembles needs to be characterized in order to model the concentrate's grade variability. Different mineralogical ensembles with similar average grades do not add to the grade variability. They can effectively be grouped together and treated as one new unit. In this way, the different facies seen in Figure 2 have been grouped according to their average copper grade. Three new ore type classifications have been created:

- high grade ore comprising chalcocite-bornite ore
- low grade ore comprising chalcopyrite and chalcopyrite-pyrite ores
- rocks that are not sent to the flotation plant. These are the remaining facies—the oxide ore (atacamite-malachite), pyrite and the barren rock that is generally found beneath the orebody.

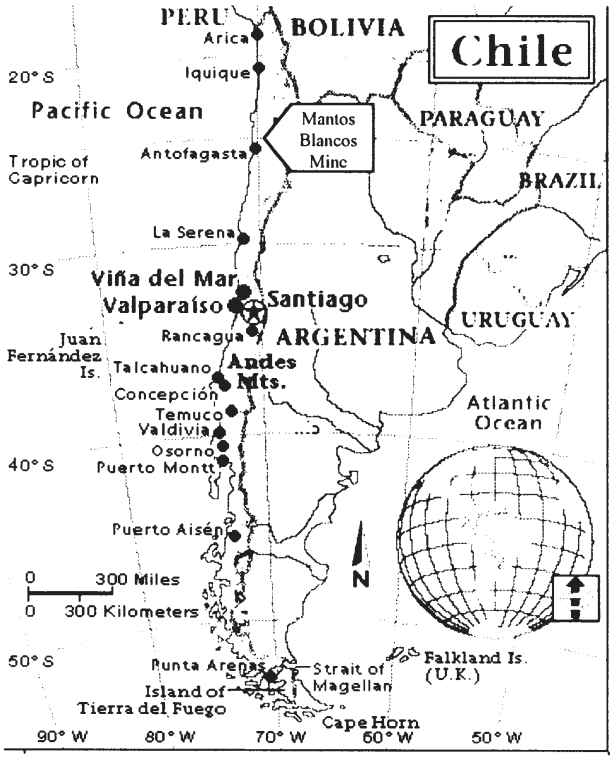

Figure 1—Location map of the Mantos Blancos mine

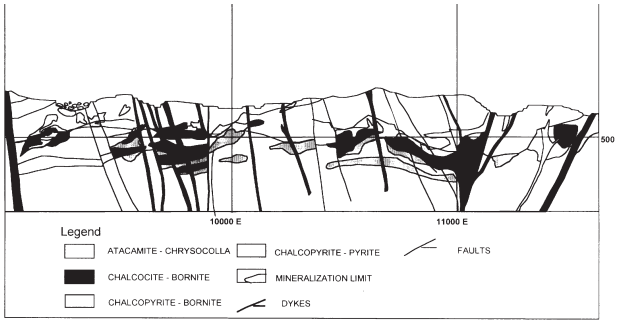

Figure 2—Typical section of the Mantos Blancos orebody

These three newly created geological units are simulated to reproduce the spatial variability of the concentrate grades. By an abuse of terminology these three geological units will be referred to as facies: the so-called high grade or *rich facies*, the low grade or *medium facies* and the non-sulphide or *poor facies*.

For this pilot study only a small part of the orebody will be dealt with. The spatial layout of the facies within this part is considered as being representative of the type of behaviour seen globally. For illustrative purposes a two-dimensional case study is presented, considering a single section through the orebody: a typical east-west section (cf. Figure 3) was chosen to provide the conditioning data. The size of the zone considered is 290 m east-west by 350 m vertically. There are 903 samples that have been taken every 2 m, mainly from vertical exploration drillholes. The drillholes are about 15 m apart in the east-west direction. The few isolated samples seen in Figure 3 come from intersecting underground development drillholes. In this Figure the three different facies are presented in different tones, light grey to the non-sulphide (waste or oxide) material, middle grey to the low-grade ore, and black to the high-grade ore. The data clearly shows the highly variable nature of the geology: it is not unusual to go from high to low grade ore and back again within the space of a few metres. It is this type of behaviour that the mine planners need to better understand in their planning.

A first glimpse at this data set allows us to identify some of the characteristics that need to be respected by the plurigaussian simulation. The systematic presence of non-sulphide material near the surface corresponds to the oxide ore or waste. Likewise, although not clearly seen in this Figure, the orebody is delimited below by barren rock. Also, given the nature of the deposit, the high grade ores are more likely to occur toward the centre of the mineralized zone. These physical constraints must be incorporated in the plurigaussian simulation technique for it to provide realistic possible images of the geology.

While this data will be used to condition the simulation,

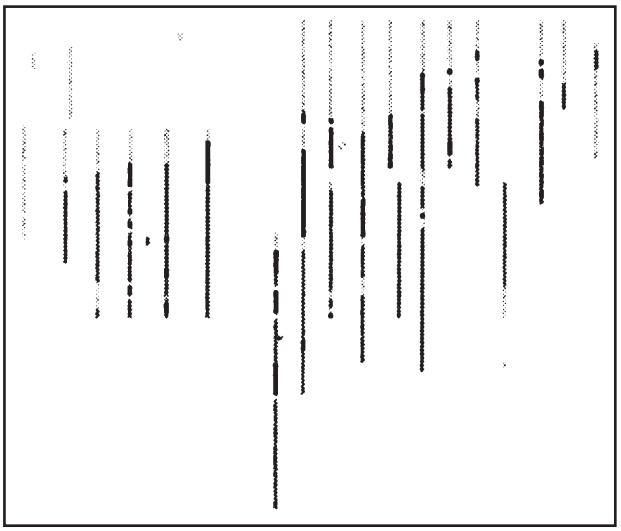

Figure 3—Samples from high (black), low (middle grey) and poor grade ore (light grey)

data for the variographic analysis comes from the same zone but defined over 5 such consecutive east-west sections. There are 8552 samples available that have been taken over a volume covering 60 m in the north-south direction that encompasses the section seen in Figure 3. Using a larger data set allows us to obtain variogram models that are representative of the global behaviour of the facies. The final facies simulations will respect the global spatial continuity of the rock types, via the variographic analysis, but will be conditioned locally to the data seen in Figure 3.

Properties of indicator variables

Indicator variables are used to define whether a given point lies within a certain facies. The indicator variable takes the value 1 if the point belongs to the facies in question or zero otherwise. Three indicator variables are required for this study, one for each facies. Jointly simulating the three indicators is therefore equivalent to simulating the geometry of the facies. For a given point $\boldsymbol{x}$, the three indicators are defined as follows:

$$\begin{aligned} \boldsymbol{I}_r(\boldsymbol{x}) &= \begin{cases} 1 & \text{if } \boldsymbol{x} \text{ is in rich ore} \\ 0 & \text{otherwise} \end{cases} \\ \boldsymbol{I}_m(\boldsymbol{x}) &= \begin{cases} 1 & \text{if } \boldsymbol{x} \text{ is in low ore} \\ 0 & \text{otherwise} \end{cases} \\ \boldsymbol{I}_p(\boldsymbol{x}) &= \begin{cases} 1 & \text{if } \boldsymbol{x} \text{ is in non-sulphide} \\ 0 & \text{otherwise} \end{cases} \end{aligned} \quad [1]$$

where $\mathbf{x} = (x,z)$ is a point in our 2D working space.

From [1] the mean of an indicator is simply the probability that the point lies in that facies. Because an indicator squared is equal to itself, the variance of an indicator is a function of its mean. For example if $E\{\mathbf{I}_r(\mathbf{x})\} = \Pr\{\mathbf{x} \text{ is in rich ore}\} = p_r(\mathbf{x})$ denotes the mean of the high ore indicator, then its variance equals:

$$Var\{\boldsymbol{I}_r(\boldsymbol{x})\} = E\{\boldsymbol{I}_r(\boldsymbol{x})^2\} - [E\{\boldsymbol{I}_r(\boldsymbol{x})\}]^2 = E\{\boldsymbol{I}_r(\boldsymbol{x})\} - p_r(\boldsymbol{x})^2 = p_r(\boldsymbol{x}) - p_r(\boldsymbol{x})^2 \quad [2]$$

So the spatial average of the indicators is the average probability representing the proportion of that type of facies in the study field. The statistics of the three indicators are given in Table I.

Globally, that is over the whole field, there is almost 10% of high grade ore and about 45% of both low grade and non-copper sulphide material. There is, however, nothing to say that these proportions should be constant in space. For example, there is much more poor grade material—in the form of oxide ore—near the top of the orebody. Lower proportions of poor and high grade ores there are compensated for by the increase in the proportion of non-copper sulphide (for flotation purposes) near the surface.

This balance of proportions reflects the important property that any one point belongs to one and only one

Table I

Statistics of indicator variables

	I_r	I_m	I_p
No. of samples	8552	8552	8552
Mean	0.0973	0.4502	0.4525
Variance	0.0878	0.2475	0.2477

facies: the point is either in the high grade ore, in the low grade ore or in the non-copper sulphide rock. This means that at any point the sum of the three indicators is equal to one:

$$\boldsymbol{I}_r(\boldsymbol{x}) + \boldsymbol{I}_m(\boldsymbol{x}) + \boldsymbol{I}_p(\boldsymbol{x}) = 1 \quad \forall \boldsymbol{x} \qquad [3]$$

This is reflected by the fact that the sum of the indicator means equals one. That is, the sum of the proportions at any point in space equals one. This point will be looked at in more detail below when defining the proportion curves.

It is this relationship, the complementary property of the facies indicators, which must be respected in all that follows to obtain consistent joint indicator simulations. At the same time this relationship means that only two of the three indicators are worked on simultaneously. The third one is automatically deduced from the first two using the relationship [3].

Traditional simulating techniques

The traditional simulation techniques for indicators are too limited to be applied to our case study. The *sequential indicator simulation* method is based on the use of a random path through the field to sequentially simulate each node of the simulation grid. For the current node the indicator is firstly cokriged from those points already simulated and the conditioning data. The resulting estimate is assumed to represent an estimate of the probability that the node belongs to the different facies. It is converted to a simulated indicator according to where a drawn random number falls within the estimated cumulative probability distribution. The major pitfall in applying this technique to the case study comes from the cross covariance model required for the cokriging step. Direct and cross indicator covariances must satisfy a certain number of conditions[9,10] for a valid cross covariance model to be defined. Some of these conditions have been presented in the Appendix. To avoid this very difficult step, an intrinsic correlation model is often assumed. All direct and cross covariances are assumed to be proportional to one underlying covariance model, which reduces the cokriging to kriging. However, this is not possible in our case due to the different spatial structures of the high and low grade facies as seen below in the variographic analysis section. The lack of a valid cross covariance model means that the sequential indicator simulation method cannot be applied to Mantos Blancos.

On the other hand a valid indicator cross covariance model is automatically defined in the framework of the *truncated gaussian* method. This method is based on the notion that the indicators are obtained by truncating one standard multigaussian random variable at different thresholds that are calculated from the known means of the various indicators. The indicator covariance model is determined by the covariance of the gaussian variable that is fixed according to an iterative process as the one that leads to the best fit of the experimental indicator covariances. An indicator simulation is obtained by truncating the corresponding conditional multigaussian simulation. This technique is limited however by the fact that all indicators are based on only one multigaussian variable and their direct and cross covariances are necessarily linked to the covariance of that variable. For this reason the truncated gaussian method has had a good deal of success in the petroleum industry where the host rock is sedimentary and different facies all present the same type of spatial behaviour. For our case study however, a double anisotropy seen during the variographic analysis stage prevents us from successfully applying this method. A more general method capable of dealing with facies that present different spatial behaviours is required. The plurigaussian simulation method is such a technique.

The plurigaussian simulation method

This method is an extension of the truncated gaussian method but based on the simultaneous truncation of several multigaussian variables thus allowing the simulation of different facies displaying different spatial anisotropies. Only a few results concerning this technique are presented here. The interested reader will find more details in the Aappendix.

As much geological knowledge as possible must be used in the construction of a plurigaussian model. It must be remembered that the underlying gaussian variables do not exist in practice: they are an intermediary mathematical tool used to obtain a consistent cross covariance model for the indicators. For the current case study, the plurigaussian model will be based on two independent multigaussian variables. The first, denoted by $Y_1 \sim N(0,1)$, is truncated so as to distinguish between the high grade and the low grade ore. This truncation will then be overprinted by the appearance of the poor grade oxide ore. The second gaussian variable, $Y_2 \sim N(0,1)$, will present a single truncation between the low grade ore and the other two facies, irrespective of whether it is low or high grade ore. This truncating process is illustrated in Figure 4(a) which shows the scatter diagram between the independent Y_1 and Y_2.

The threshold values for Y_1 and Y_2 are t_1 and t_2 respectively. It can be seen how the truncation of Y_2 seems to have overprinted the earlier truncation of Y_1 — the dashed part of the line at the threshold t_1. The two independent gaussian variables vary roughly between -3 and 3. Figure 4(b) is the corresponding colour representation of the truncation with poor ore shown in light grey, low ore in middle grey and high grade ore in black. The thresholds used here are those corresponding to the global proportions seen in Table I. Truncating these variables creates 'patches' of either high or low values whose continuity depends on the continuity of the

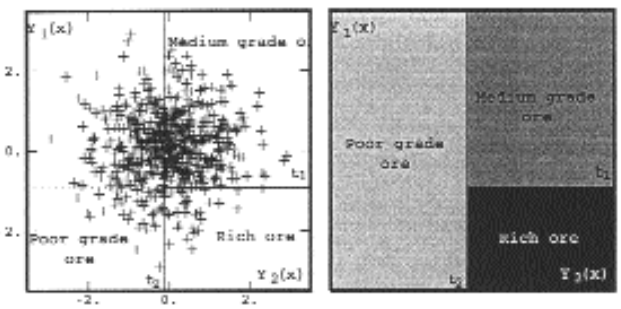

(a) Scatter diagram (b) Colour representation

Figure 4—Truncation of two independent multigaussian variables

gaussian variables. These 'patches'", coded as indicators, are created so as to mimic the spatial behaviour of the different facies of the ore unit. So the way that the two gaussian variables are truncated mathematically defines the three indicators:

$$\begin{aligned} \boldsymbol{I}_p(\boldsymbol{x}) &= \begin{cases} 1 & Y_2(\boldsymbol{x}) < t_2(\boldsymbol{x}) \\ 0 & \text{otherwise} \end{cases} \\ \boldsymbol{I}_m(\boldsymbol{x}) &= \begin{cases} 1 & Y_2(\boldsymbol{x}) \geq t_2(\boldsymbol{x}) \text{ and } Y_1(\boldsymbol{x}) \geq t_1(\boldsymbol{x}) \\ 0 & \text{otherwise} \end{cases} \\ \boldsymbol{I}_r(\boldsymbol{x}) &= \begin{cases} 1 & Y_2(\boldsymbol{x}) \geq t_2(\boldsymbol{x}) \text{ and } Y_1(\boldsymbol{x}) < t_1(\boldsymbol{x}) \\ 0 & \text{otherwise} \end{cases} \end{aligned} \quad [4]$$

From the scatter diagram, changing the value of the threshold increases or decreases the number of points assigned to a given facies, that is the proportion of each facies that is known from the experimental data. The value of the thresholds is in fact determined by the proportion of each facies. For example, from Equations [2] and [4] the thresholds can be calculated using:

$$\begin{aligned} E\{\boldsymbol{I}_p(\boldsymbol{x})\} &= p_p(\boldsymbol{x}) = \Pr\{Y_2(\boldsymbol{x}) < t_2(\boldsymbol{x})\} = G(t_2(\boldsymbol{x})) \\ E\{\boldsymbol{I}_m(\boldsymbol{x})\} &= p_m(\boldsymbol{x}) = \Pr\{Y_2(\boldsymbol{x}) \geq t_2(\boldsymbol{x}) \text{ and } Y_1(\boldsymbol{x}) \geq t_1(\boldsymbol{x})\} = \{1 \pm G(t_1(\boldsymbol{x}))\} \times \{1 \pm G(t_2(\boldsymbol{x}))\} \end{aligned} \quad [5]$$

where G is the known standard gaussian cumulative distribution function. So once the indicator means have been modelled, the preceding Equations are inverted to calculate firstly t_2 then t_1.

Modelling facies proportions

Assuming constant facies proportions over the entire field corresponds to supposing that the indicators are stationary because their mean is constant in space. If these means, or equivalently the facies proportions, are constant in space then the threshold values are also constant. As specified by Equation [9] the indicator covariance function only depends on the distance separating the points. This is certainly not the case here where it is known for example that there is only oxide (poor grade) ore near the surface of the deposit. The facies proportions must therefore be modelled as a function of the point considered in the field. This modelling procedure is guided by the experimental data and by the geological understanding of the orebody considered. As a first pass approach a simple moving average of the experimental indicator values over the study field is considered. This can then be refined and complemented manually to incorporate knowledge about the geological characteristics of the site. This is the case in particular for the poor ore at the bottom part of the field where there is little or no data but where information from neighbouring areas suggest that this part of the field is essentially made of poor ore in the form of barren rock.

These characteristics can be seen in Figure 5 that presents some of the so-called proportion curves. In this Figure the proportion of the three facies is shown as a coloured surface on the vertical axis: high grade ore in black, low ore in middle grey and poor grade in light grey. The sum of the facies proportions is always equal to 100%. The horizontal axes are the east-west direction (on the left) and the vertical direction (on the right). Figure 5(a) shows the horizontal proportion curve close to the surface, and the vertical proportion curve from the western side of the field. Figure 5(b) shows both the horizontal and vertical proportion curves closer to the centre of the field. From these curves it can be seen how the characteristics mentioned in the previous paragraph have been taken into account and in particular how the proportion of low and poor facies can vary significantly over a relatively small distance. The proportion of high grade ore seems more regular as it is essentially limited to the central part of the field. Once the facies proportions have been modelled the corresponding threshold values t_1 and t_2 are calculated at each point in space from Equation [5] and before going on to the indicator variographic analysis step.

Variographic analysis of indicators

The plurigaussian technique provides a valid indicator cross covariance model because the indicator covariances are directly deduced from the covariance model of the gaussian variables. Assigning a standard covariance model (for example spherical, exponential or gaussian) to Y_1 and Y_2 guarantees that the indicator covariances are valid covariance functions. The two gaussian variables will be assumed to have stationary covariances:

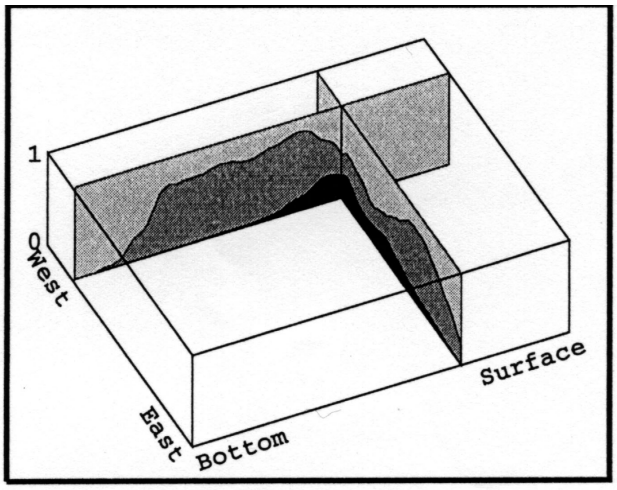

(a) surface and western edge

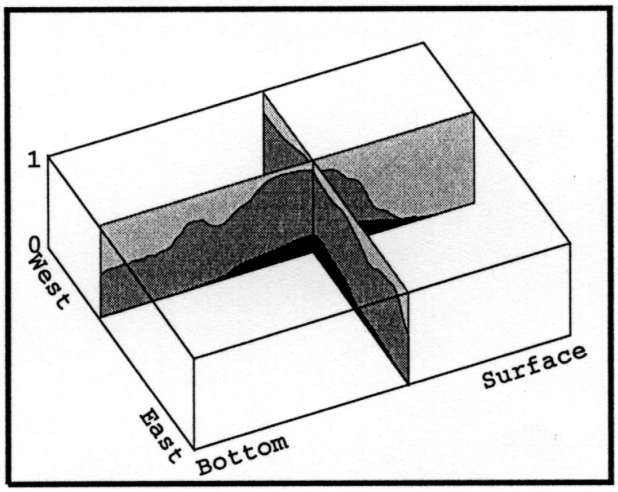

(b) Centrally located

Figure 5—Horizontal and vertical lithofacies proportion curves

$$Cov\{Y_1(\boldsymbol{x}),Y_1(\boldsymbol{x}+\boldsymbol{h})\} = \rho_1(\boldsymbol{h}) \text{ and } Cov\{Y_2(\boldsymbol{x}),Y_2(\boldsymbol{x}+\boldsymbol{h})\} = \rho_2(h) \quad [6]$$

For convenience sake it was decided to perform the variographic analysis step on the direct and cross indicator variograms and not on the covariances. Let us take the example of the poor ore indicator variogram, denoted by $\gamma_p(\mathbf{x},\mathbf{h})$. It can be shown that this variogram, like the indicator mean, depends on the point $\mathbf{x}$:

$$\gamma_p(\boldsymbol{x},\boldsymbol{h}) = \frac{1}{2}\left\{p_p(\boldsymbol{x}) + p_p(\boldsymbol{x}+\boldsymbol{h}) - 2E\left\{\boldsymbol{I}_p(\boldsymbol{x})\boldsymbol{I}_p(\boldsymbol{x}+\boldsymbol{h})\right\}\right\} \quad [7]$$

Given that the mean $p_p(\mathbf{x})$ is known, only an explicit expression for the non-centred indicator covariance must be obtained from the indicator definition in [4] in order to calculate the value of the non-stationary indicator variogram:

$$E\left\{\boldsymbol{I}_p(\boldsymbol{x})\boldsymbol{I}_p(\boldsymbol{x}+\boldsymbol{h})\right\} = \Pr\left\{Y_2(\boldsymbol{x}) < t_2(\boldsymbol{x}) \text{ and } Y_2(\boldsymbol{x}+\boldsymbol{h}) < t_2(\boldsymbol{x}+\boldsymbol{h})\right\} \quad [8]$$

where, as previously specified, Y_2 is a not only gaussian but also multigaussian. So this probability can be calculated as an area under the bigaussian probability density function denoted by $g(u, v, \rho_2(\mathbf{h}))$:

$$E\left\{\boldsymbol{I}_p(\boldsymbol{x})\boldsymbol{I}_p(\boldsymbol{x}+\boldsymbol{h})\right\} = \int_{-\infty}^{t_2(\boldsymbol{x})} du \int_{-\infty}^{t_2(\boldsymbol{x}+\boldsymbol{h})} g\left(u,v,\rho_2(\boldsymbol{h})\right)dv \quad [9]$$

which provides the final step in the calculation of the poor ore indicator variogram. The indicator variograms for the low grade and high grade ores as well as the cross variograms are obtained in a similar fashion as shown in the Appendix.

In practical terms the experimental indicator direct and cross variograms are calculated from the facies data. From these experimental variograms the covariance model of the two underlying gaussian variables must be found. To do so, an iterative approach with the following steps is used:

(i) Calculate the direct and cross experimental indicator variograms
(ii) Choose an initial covariance model of the two underlying multigaussian variables
(iii) Calculate the corresponding direct and cross indicator variogram model
(iv) IF the indicator variogram model does not fit the experimental indicator variograms THEN modify the covariance model of the two gaussian variables and go to step (iii)
(v) Retain the chosen covariance model for the gaussian variables.

An initial covariance model is assigned to each of the gaussian variables based for example on the main directions of anisotropy seen in the experimental indicator variograms. If the resulting fit of the experimental variograms is not satisfactory then the gaussian covariance model is changed accordingly. The procedure is repeated until a satisfactory fit is obtained. For our case study Figure 6 presents the finally accepted fit of the experimental direct and cross indicator variograms. The dotted line is the experimental variogram and the thick continuous line the fitted model. It must be remembered that these are in fact the average non-stationary indicator variogram values (experimental and model) calculated at the location of the data points. The maximum distance shown is equal to about half the width of the field.

The experimental variograms are calculated along the main directions of anisotropy—dipping about 70° east and 20° west for the high grade ore and about 20° degrees east and 70° degrees west for both the poor and low grade ore. The fit is satisfactory in all directions and for all the variograms. The different heights reached by the various indicator variograms reflects the differing proportions between the various facies, there being about the same amount of poor and low grade ore and much less high grade ore. The difference in height between the indicator variogram model and the experimental indicator variograms is explained by a difference in the experimental proportions and the modelled proportions. This is most notable for the high grade ore when a small change in a low proportion value leads to a significant change in the height of the variogram. Not surprisingly the poor and low grade ore display very similar anisotropic behaviour given that they are almost complementary indicators because of the low proportion of high grade ore.

For Mantos Blancos, there is a certain amount of flexibility in the choice of variogram model assigned to the two gaussian variables. While the different indicator anisotropies are directly determined by the equivalent anisotropies of the gaussian variogram models, assigning different types of structures (spherical, exponential, gaussian, cubic etc.) to the gaussian variables can sometimes lead to very similar fits of the experimental indicator variograms. This is particularly the case for the variograms of the low and poor ore indicators that may for example be modelled equally well by assigning either with a small nugget effect or a small scale structure to the variable Y_1. Non-conditional indicator simulations can be used to help decide which of these two possible gaussian variogram models should be retained. The model that leads to the most pleasing non-conditional simulation (that is, the one that looks most like what has been observed in practice, or what is known about the deposit) is the one that is retained.

Figure 7 shows two such non-conditional simulations that have been obtained from the same variogram model of Y_1 but two different variogram models for Y_2. Assigning a small nugget effect and a large-scale gaussian structure to Y_2 led to Figure 7(a). Then replacing the nugget effect by a small-scale gaussian structure led to Figure 7(b). These two

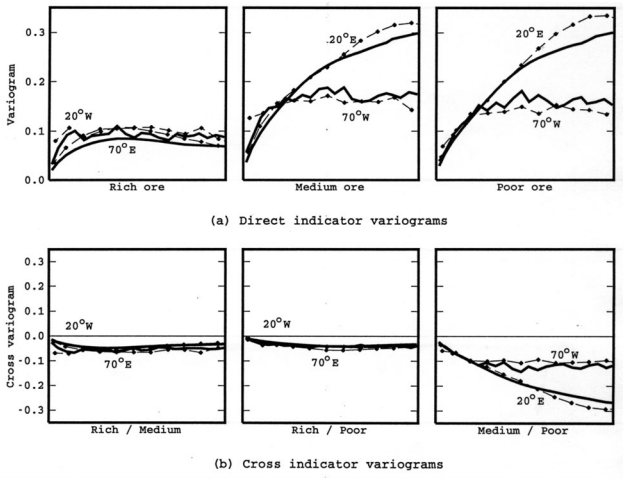

Figure 6—Experimental indicator variograms and the fitted model

Figures differ by the type of contact between the low and poor ores, shown in middle and light grey respectively. Including the nugget effect leads to a very spotty transition zone between these ores whereas the small-scale gaussian structure produces small flame-like shoots of low grade ore into the poor ore. It is this second type of spatial behaviour that is most consistent with what has been observed in the mined out parts of the deposit. So the second variogram model, including the small-scale gaussian structure, has been retained for the variable Y_2. A similar type of test was performed for the second variable Y_2 to determine which type of variogram model provides the right contact between the high grade and low grade ores.

The final choice of the gaussian variable variogram model can be based not only on a good fit of the experimental indicator variograms but also on a subjective appreciation of the consistency of non-conditional simulations with respect to what is known about the geology of the deposit. In this way a single spherical covariance structure was assigned to the second gaussian variable Y_2 that essentially separates the high grade ore from the low grade ore. The variable Y_1, that divides the poor from the other ores, was assigned two gaussian structures: a small scale one—5% of the total variability—and one with a long range defining the overall spatial behaviour of the indicator. The final variogram models chosen for the underlying gaussian variables are shown in Figure 8. The directions shown correspond to the main directions of anisotropy that are also the main directions of anisotropy of the indicators themselves. The distance scale shown here is the same as that seen in Figure 6 for the indicator variograms and

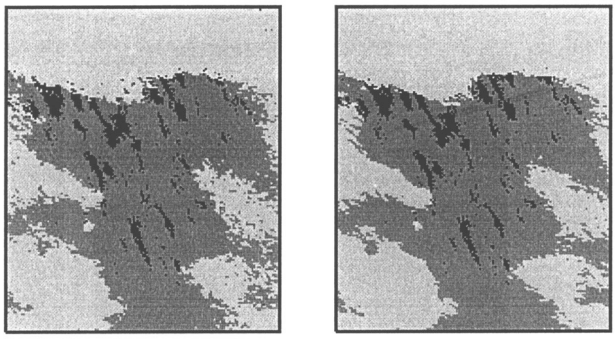

(a) With nugget effect (b) With gaussian structure

Figure 7—Non-conditional plurigaussian simulations

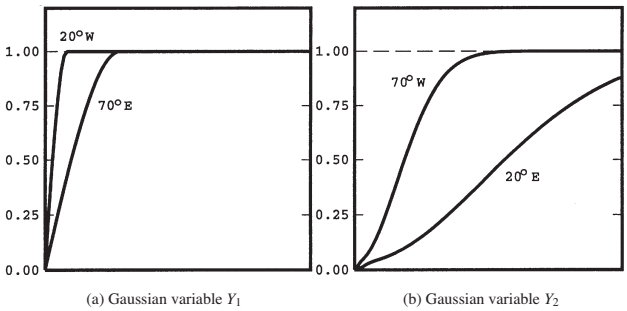

(a) Gaussian variable Y_1 (b) Gaussian variable Y_2

Figure 8—Variogram model for the two independent gaussian variables

vertically the models reach a sill of one as standard multigaussian variables are being used. As expected, there are obvious similarities between the variogram model of Y_1 and the high grade ore indicator variogram model. For the low and poor ores the link between the relevant gaussian and indicator variogram models is less obvious because of the indicator variogram calculated at 70°W does not reach the same sill as that calculated in the perpendicular direction.

Conditional simulation

Having assigned a covariance model to the gaussian variables, it is possible to go on to the simulation step. The simulation of the facies is based on the simulation of the two multigaussian variables Y_1 and Y_2 using a standard multigaussian simulation technique, like the turning bands method or sequential gaussian simulations. At each point of the simulated multigaussian field and the two gaussian variables are truncated according to [3] so as to obtain the simulated facies for that point. The mineralogical data, that is the indicator data seen in Figure 3, will be used to condition the simulation algorithm to the zone under study. At each point, this indicator information provides an interval, defined by the thresholds t_1 and t_2, in which the value of the two gaussian variables must lie according to the type of ore observed there.

To perform a conditional simulation of the gaussian variables, experimental multigaussian values are required at the data points. To obtain these values, that respect the gaussian covariance models, the multigaussian spatial distribution and the intervals imposed by the thresholds, a Gibbs sampler algorithm[11,12,13] is used. This is an iterative algorithm that starts by assigning randomly drawn standard gaussian values to all of the experimental points. Each point is then kriged from the remaining points and a new value is assigned to the kriged point that satisfies the applicable threshold values. Consider the example of the experimental point $\mathbf{x}_0$ that lies in the high grade ore. Then the new values of Y_1 and Y_2 that are assigned to this experimental point are defined as follows:

$$\begin{aligned} Y_1(\boldsymbol{x}_0) &= Y_1^{SK}(\boldsymbol{x}_0) + \sigma_{1,SK}(\boldsymbol{x}_0)U(\boldsymbol{x}_0) \\ Y_2(\boldsymbol{x}_0) &= Y_2^{SK}(\boldsymbol{x}_0) + \sigma_{2,SK}(\boldsymbol{x}_0)V(\boldsymbol{x}_0) \end{aligned} \quad [10]$$

where $Y_1^{SK}(\mathbf{x}_0)$ and $Y_2^{SK}(\mathbf{x}_0)$ are the simple kriging estimates of $Y_1(\mathbf{x}_0)$ and $Y_2(\mathbf{x}_0)$ respectively, $\sigma_{1,SK}(\mathbf{x}_0)$ and $\sigma_{1,SK}(\mathbf{x}_0)$ the corresponding simple kriging standard deviations, and $U(\mathbf{x}_0)$, $V(\mathbf{x}_0) \sim N(0,1)$ two independent standard gaussian variable that lie in the intervals defined by the threshold values. Because the point $\mathbf{x}_0$ lies in the high grade ore, it is known from Equation [4] that $Y_2(\mathbf{x}_0) \geq t_2(\mathbf{x}_0)$ and $Y_1(\mathbf{x}_0) < t_1(\mathbf{x}_0)$. $U(\mathbf{x}_0)$ and $V(\mathbf{x}_0)$ must therefore satisfy:

$$\begin{aligned} U(\boldsymbol{x}_0) &< \frac{t_1(\boldsymbol{x}_0) - Y_1^{SK}(\boldsymbol{x}_0)}{\sigma_{1,SK}(\boldsymbol{x}_0)} \\ V(\boldsymbol{x}_0) &\geq \frac{t_2(\boldsymbol{x}_0) - Y_2^{SK}(\boldsymbol{x}_0)}{\sigma_{2,SK}(\boldsymbol{x}_0)} \end{aligned} \quad [11]$$

Values of $U(\mathbf{x}_0)$ and $V(\mathbf{x}_0)$ satisfying this condition are randomly drawn and $Y_1(\mathbf{x}_0)$ and $Y_2(\mathbf{x}_0)$ are updated according to Equation [10]. The next experimental point is then updated in the same way. It has been shown that after

many passes through all the experimental points the resulting series of Y_1 and Y_2 values are indeed standard multigaussian with the desired covariance model while respecting the thresholds imposed by the facies proportions.

An example of the procedure is presented for one of the central drillholes of Figure 3 that has been reproduced in Figure 9(a) in the form of logged facies where, as usual, the high grade ore is shown in black, the low grade ore in middle grey and the non-sulphide material in light grey. From the proportion curves the value of the thresholds along the drillhole is known after having inverted Equation [5]. These threshold values restrict the possible range of gaussian values along the drillhole as is respected by the Gibbs sampler algorithm. Figure 9(b) shows the gaussian Y_1 (thick line) and its threshold t_1 (grey filled curve) along the drillhole. The low threshold values near the surface correspond to the fact that there is no high grade ore there. The truncation $Y_1 < t_1$ is then applied to reconstruct the drillhole (right hand side) in terms of low and high grade ores. The realisation of Y_2 and its threshold t_2 are presented in Figure 9(c). Setting a very high threshold toward the surface virtually ensures that only poor (oxide) ore is simulated there. This gaussian variable is less variable down the drillhole as expected from the longer range of its variogram model in the vertical direction when compared with Y_1. To confirm that the realisation of Y_2 is valid the truncation is applied to create the poor ore indicator (right hand side) down the drillhole. If this reconstructed poor ore indicator then overprints the existing low and high grade ores the resulting configuration is found to match the experimental data as required.

The gaussian values that are assigned to the drillholes in this way are used as conditioning data for the conditional simulation of Y_1 and Y_2. Note that all the experimental data are treated simultaneously by the Gibbs sampler algorithm so that all the correlations between samples from different drillholes as well-along the same drillhole are respected. The plurigaussian simulation of the facies is finally obtained by truncating a multigaussian simulation according to [4]. The four examples of such simulations, presented in Figure 10, show that the simulation technique respects both this conditioning data and the proportions of the different facies. There is always a crowning layer of poor (oxide) ore that butts onto both high and low grade ore. The greatest concentration of high grade ore is towards the centre of the zone as is consistent with the porphyry nature of the deposit and toward the bottom of the field the barren rock becomes more frequent there where it delimits the mineralized ore.

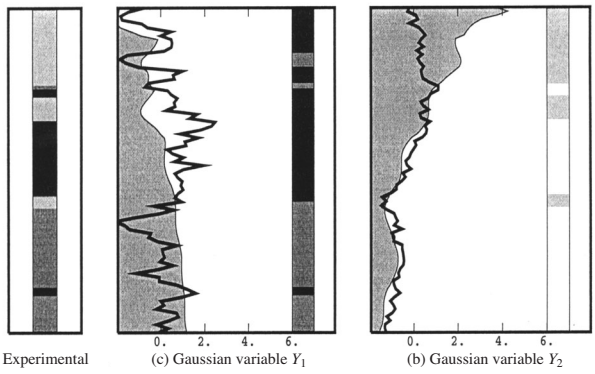

Figure 9—Obtaining the gaussian conditioning data from indicator data

Conclusions

For the test case presented here, a porphyry copper deposit in Chile, it was seen that simulating the different facies using traditional indicator simulation methods was not possible because these methods are either too limited in their applicability or too difficult to put into practice. This is because the facies behave differently in space; the high grade ore seems to be almost vertically continuous while the low grade and non-sulphide material are closer to being horizontally continuous. These different anisotropies can only be taken into account by the very general plurigaussian simulation method. This method was shown to be very effective in reproducing the characteristics of the different facies not only their orientation, but also their distribution across the studied area as determined by the proportion of each rock type.

This, however, is just one of the many possible applications of the plurigaussian method. By its very construction, this method is potentially a very powerful tool for simulating a variety of different types of orebody. Geological expertise must be incorporated in the construction of the plurigaussian model to define what constraints regarding the spatial distribution of the rock types must be respected; certain facies not touching others or inversely always adjoining other given facies for example. Taking account of such constraints allows us to produce more realistic scenarios of the geometry of an orebody and hence to have a greater understanding of the orebody itself.

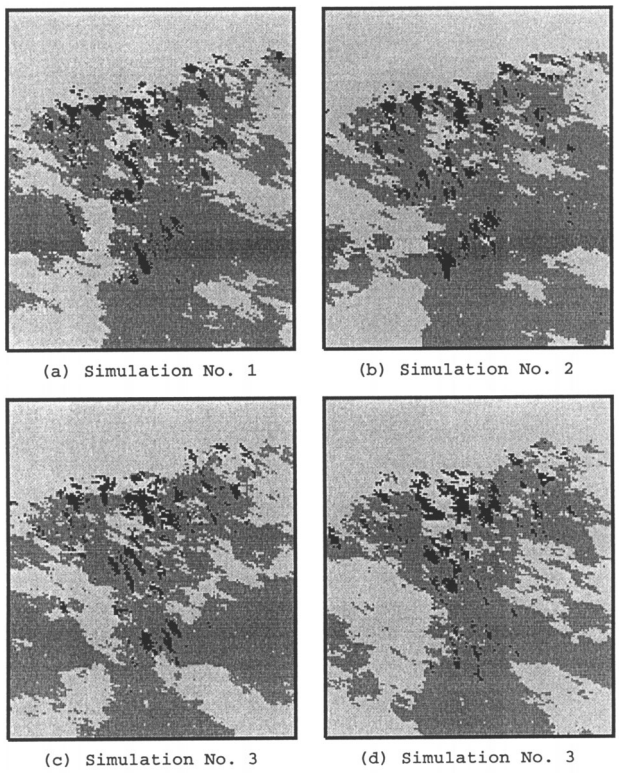

Figure 10—Conditional plurigaussian simulations

Knowing more about an orebody makes it easier to exploit it profitably.

Appendix

Some results concerning indicators and indicator covariances[5,8,9] are presented here. In particular the relationships that must be taken into account when developing a valid direct and cross covariance model will be dealt with. Results for the 3 indicator case ($\mathbf{I}_r$,$\mathbf{I}_m$ and $\mathbf{I}_p$), corresponding to the case study used, will be presented. These results can be generalized when more indicators are considered. Let C_r,C_m, $C_{r,m}$ etc. denote the direct and cross centred covariances of the indicators. Because $\mathbf{I}_r + \mathbf{I}_m + \mathbf{I}_p = 1$ the following relationships must be respected by the indicator covariance model:

$$\begin{aligned} C_r(\boldsymbol{h}) &= -C_{r,m}(\boldsymbol{h}) - C_{r,p}(\boldsymbol{h}) \\ C_m(\boldsymbol{h}) &= -C_{m,r}(\boldsymbol{h}) - C_{m,p}(\boldsymbol{h}) \\ C_p(\boldsymbol{h}) &= -C_{p,r}(\boldsymbol{h}) - C_{p,m}(\boldsymbol{h}) \\ C_{r,m}(\boldsymbol{h}) - C_{m,r}(\boldsymbol{h}) &= C_{m,p}(\boldsymbol{h}) - C_{p,m}(\boldsymbol{h}) = C_{p,r}(\boldsymbol{h}) - C_{r,p}(\boldsymbol{h}) \end{aligned} \quad [A1]$$

These results apply to both stationary and non-stationary indicators in which case the covariances depend on both $\mathbf{x}$ and $\mathbf{h}$, despite the slightly abusive notation above. A further condition on any indicator variogram is that it must satisfy the following so-called triangular inequality:

$$\gamma_r(\boldsymbol{h}_1 + \boldsymbol{h}_2) \le \gamma_r(\boldsymbol{h}_1) + \gamma_r(\boldsymbol{h}_2) \quad [A2]$$

from which it is deduced that near the origin the variogram must increase as a function of $|\mathbf{h}|^{\alpha}$ where $\alpha \le 1$, thus excluding gaussian covariances for example. So it is very difficult to fit a valid covariance model even to only 3 indicators simultaneously. The truncated gaussian or plurigaussian working framework guarantee that these and all other necessary conditions are met. A valid indicator covariance model is obtained because all direct and cross indicator non-centred covariances are calculated from the gaussian counterpart as in Equation [9] for the poor ore indicator. For the high grade ore indicator covariance and the cross covariance between poor and high grade ore indicators it is found that:

$$E\{\boldsymbol{I}_r(\boldsymbol{x})\boldsymbol{I}_r(\boldsymbol{x}+\boldsymbol{h})\} = \int_{t_2(x)}^{\infty} du \int_{t_2(x+h)}^{\infty} g(u,v,\rho_2(\boldsymbol{h}))dv \int_{-\infty}^{t_1(x)} ds \int_{-\infty}^{t_1(x+h)} g(s,t,\rho_1(\boldsymbol{h}))dt \quad [A3]$$

$$E\{\boldsymbol{I}_p(\boldsymbol{x})\boldsymbol{I}_r(\boldsymbol{x}+\boldsymbol{h})\} = G(t_1(\boldsymbol{x}+\boldsymbol{h})) \int_{-\infty}^{t_2(x)} du \int_{t_2(x+h)}^{\infty} g(u,v,\rho_2(\boldsymbol{h}))dv \quad [A4]$$

where the gaussian cumulative density and the bigaussian probability density functions are:

$$G(t) = \frac{1}{\sqrt{2\pi}} \int_{-\infty}^{t} e^{-u^2/2} du \text{ and } g(u,v,\rho) = e^{-\left(\frac{u^2+v^2-2uv\rho}{2(1-\rho^2)}\right)} / 2\pi\sqrt{1\pm\rho^2} \quad [A5]$$

respectively. While the direct indicator variograms are calculated as in Equation [7], the cross variograms are obtained as follows:

$$\gamma_{p,r}(\boldsymbol{x},\boldsymbol{h}) = -\frac{1}{2}\left\{E\{\boldsymbol{I}_p(\boldsymbol{x})\boldsymbol{I}_r(\boldsymbol{x}+\boldsymbol{h})\} + E\{\boldsymbol{I}_p(\boldsymbol{x})\boldsymbol{I}_r(\boldsymbol{x}+\boldsymbol{h})\}\right\} \quad [A6]$$

References

1. Alabert, F. Stochastic imaging of Spatial Distributions using Hard and Soft Data, Doctorate Thesis, Stanford University, California, 1987. 197 pp.
2. Deutsch, C.V. and Journel, A.G. 1992, *GSLIB*: *Geostatistical software library and user's guide*, Oxford University Press, New York. 1992.
3. Matheron, G., Beucher, H., Fouquet, C. de, Galli, A., Guerrillot, D., and Ravenne, C. Conditional simulation of the geometry of fluvio-deltaic reservoirs, *SPE 62nd Annual Conference*, Dallas, Texas, September 27–30, SPE 16753, 1987. pp. 571–599.
4. Fouquet, C. de, Beucher, H., Galli, A., and Ravenne, C. Conditional simulation of random sets. Application to an argilaceous sandstone reservoir, *Geostatistics: Proceedings of the Third International Geostatistics Congress, Avignon, France*, 5–9 Sept. 1988, M. Armstrong, ed., Kluwer Academic Publishers, Dordrecht, 1989. pp. 517–530.
5. Galli, A., Beucher, H., Le Loc'h, G., Doligez, B., and the HERESIM Group, The pros and cons of the truncated gaussian method, *Geostatistical Simulations: Proceedings of the Geostatistical Workshop, Fontainebleau, France, 27-28 May 1993*, M. Armstrong & P. Dowd, eds, Kluwer Academic Publishers, Dordrecht, 1994. pp. 217–233.
6. Le Loc'h, G., Beucher, H., Galli, A., Doligez, B., and the HERESIM Group, Improvement in the truncated gaussian method: combining several gaussian functions, *ECMOR IV: 4th European Conference on the Mathematics of Oil Recovery,* Rφros, Norway, 7–10 June 1994, Conference Proceedings, 1994. 13 pp.
7. Le Loc'h, G. and Galli, A. Truncated plurigaussian method: theoretical and practical points of view, *Geostatistics Wollongong '96*, E.Y. Baafi and N.A. Schofield, eds, Kluwer Academic Publishers, Dordrecht, 1997. pp. 211–222.
8. Roth, C., Armstrong, M., Galli, A., and Le Loc'h, G. Using plurigaussian to reproduce lithofacies with contrasting anisotropies, *Proceedings of the 27th International Symposium APCOM'98*, Institution for Mining and Metallurgy, London, 1998. pp. 201–214.
9. Rivoirard, J. Relations between the indicators related to a regionalised variable, *Geostatistics Trioa '92*, A. Soares, ed., Kluwer Academic Publishers, Dordrecht, 1993. pp. 273–284.
10. Matheron, G. The internal consistency of models in geostatistics, *Geostatistics: Proceedings of the Third International Geostatistics Congress,* Avignon, France, 5–9 Sept. 1988, M. Armstrong, ed., Kluwer Academic Publishers, Dordrecht, 1989. pp. 21–38.
11. Geman, S. and Geman, D. Stochastic relaxation, Gibbs distribution and the bayesian restoration of images, *I.E.E.E. transactions: Pattern analysis and machine intelligence*, vol. 6, 1984. pp. 721–741.
12. Freulon, X. Conditionnement du modéle gaussien par des inégalités ou des randomisées, Doctorate thesis, Centre de Géostatistique, ENSMP, Fontainebleau, 1992. 168 pp.
13. Freulon, X. and Fouquet, C. de, Conditioning a gaussian model with inequalities, *Geostatistics Troia '92*, A. Soares, ed., Kluwer Academic Publishers, Dordrecht, 1993. pp. 201–212. ◆

New manager for Mintek's Mineralogy Division*

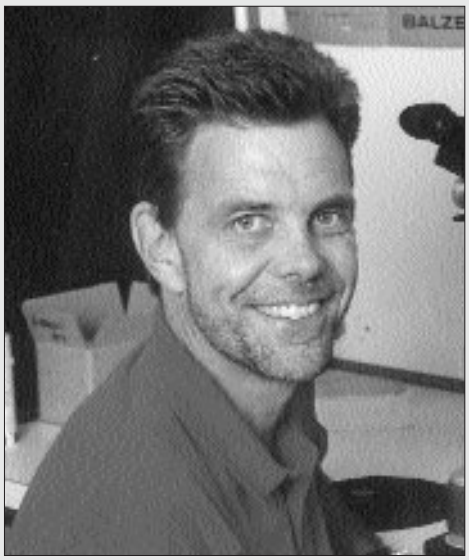

Dr Johan Nell has succeeded Dr Eduard 'Oosie' Oosthuyzen as Manager of Mintek's Mineralogy Division.

Johan, who has spent 15 years in research at Mintek, obtained his PhD at Northwestern University in Illinois, and has an extensive background in process mineralogy.

In 1994 he was awarded a Von Humboldt Fellowship for a year's post-doctoral studies at the Bayerisches Geoinstitut, University of Bayreuth in Germany.

His special interests include phase equilibria in iron-titanium oxides, and matte smelting of the platinum-group metals. ◆

* *Issued by Patricia Speedie, Specialist: Public Relations, Mintek, Private Bag X3015, Randburg 2125, Tel: (011) 709-4111, Fax: (011) 709-4326.*

Heinrich takes top spot*

Heinrich Möller is congratulated by Mintek president, Dr Aidan Edwards

Heinrich, Möller has been chosen as Mintek's top bursar for 1999.

Heinrich, who studied metallurgical engineering at the University of Pretoria, achieved an average of 85% for his three years of study. ◆

* *Issued by Patricia Speedie, Specialist: Public Relations, Mintek, Private Bag X3015, Randburg, 2125, Tel: (011) 709-4111, Fax: (011) 709-4326*

Elias excels in studies*

Elias Phasha has been chosen as Mintek's top MAP student for 1999.

Elias, who obtained an *A* for science and an *A* for maths in the IEB Senior Certificate examination, has been awarded a bursary by Mintek to study metallurgical engineering at the University of the Witwatersrand.

The Mintek MAP Programme, which has been operating since 1992, gives promising students the opportunity to upgrade their maths and science marks to enable them to embark on tertiary studies in science anf technology.

For more information on the MAP programme, contact Dr Glyn Moore at Mintek on (011) 709-4271. ◆

* *Issued by Patricia Speedie, Specialist: Public Relations, Mintek, Private Bag X3015, Randburg 2125. Tel (011) 709-4111, Fax: (011) 709-4326.*